

## Sleep Posture Recognition With a Dual-Frequency Microwave Doppler Radar and Machine Learning Classifiers

Shekh Md Mahmudul Islam<sup>1\*</sup>  and Victor M. Lubecke<sup>2\*\*</sup> 

<sup>1</sup>Department of Electrical and Electronic Engineering, University of Dhaka, Dhaka 1000, Bangladesh

<sup>2</sup>Department of Electrical Engineering, University of Hawaii at Manoa, Honolulu, HI 96822 USA

\*Member, IEEE

\*\*Fellow, IEEE

Manuscript received November 18, 2021; revised January 20, 2022; accepted January 29, 2022. Date of publication February 4, 2022; date of current version March 4, 2022.

**Abstract**—An automated, robust, noncontact sleep posture recognition technique is proposed in this letter, which uses optimizable (Bayesian hyperparameter tuning) machine learning (ML) classifiers applied to dual-frequency (2.4 GHz, 5.8 GHz) monostatic continuous-wave radar-measured effective radar cross section and chest displacement. The technique is demonstrated to accurately recognize three different key sleep postures categories for 20 participants, with greater accuracy and computational efficiency than prior published research involving either a custom ML model or threshold-based assessment. Three ML classifiers (K-nearest neighbor, support vector machine (SVM), and decision tree) were assessed, with an SVM using a quadratic kernel achieving an accuracy of 85 and 80%, at 2.4 and 5.8 GHz, respectively, and the decision tree classifier recognizing sleep postures in less than 2 min with 98.4% accuracy for dual-frequency combined measurements.

**Index Terms**—Microwave/millimeter sensors, doppler radar, machine learning (ML), radar cross section (RCS), sleep postures.

### I. INTRODUCTION

Body posture and movement during sleep correlate strongly with sleep quality and health outcomes [1], [2]. For example, sleeping in a supine posture (i.e., sleeping on one's back) can increase the risk of obstructive sleep apnea [3] and sudden infant death syndrome [4]. Prior research has focused on recognizing sleep postures mainly from wearable sensors such as those used for an electrocardiogram [5], pressure-sensitive bedsheet textile sensors [6], and video cameras [7]. The use of such sensors can interfere with the sleep behavior being measured, as contact devices worn during sleep can be uncomfortable and restrictive, whereas camera-based sensors used in a private space during sleep can cause privacy concerns [8], [9].

This letter examines an optimizable machine learning (ML) approach for sleep posture recognition, which can be assessed simultaneously during the measurement of a subject's cardiopulmonary motion pattern using a noncontact, unobtrusive microwave Doppler radar. The efficacy of Doppler radar remote sensing of cardiopulmonary activity has been demonstrated both for isolated subjects [10], [11] and small groups [12]. Prior research has also demonstrated the efficacy of unobtrusive noncontact radar-based technology for normal sleep monitoring [13], [14] and sleep apnea detection [15]. Additionally, radar has been applied for the recognition of sleep stages (i.e., rapid eye movement (REM), non-REM) [16] and sleep apnea events [17]. Recently, sleep posture recognition has also been investigated using frequency-modulated continuous wave (FMCW) radar with a multipath analysis of reflections used to distinguish sleep postures for healthy people using a custom ML (neural network) model [18]. However, the proposed method requires adding a new transfer learning model for different subjects and environments for which multipath is highly dependent. Additionally, system accuracy degrades from

94.1 to 86.7 and 83.7% due to changes in the environment even after integrating new transfer learning models. Therefore, a robust ML model is required, which can adapt its parameters automatically with changes in the dataset.

In Doppler radar measurements, the reflected phase-modulated signal varies in direct proportion to the minute movement of the chest surface due to cardiorespiratory activity. The power of the reflected signal at the receiver is a measure of the effective radar cross section (ERCS) of the target [19], [20]. When people switch sleep postures the ERCS is affected due to the asymmetric shape of the body as different portions are exposed to the radar signal. The fundamental theory introducing ERCS with dual-frequency (2.4 and 5.8 GHz) measurements related to different sleep postures has been reported in a Ph.D. dissertation along with a proposed threshold-based decision algorithm, which assesses posture based on a cumbersome statistical analysis across three key categories of posture assumed (supine, prone, and side), with supine taken as a reference [19], [20]. The proposed threshold-based decision algorithm worked without error for 78% of the subjects using 2.4 GHz, 65% using 5.8 GHz, and 100% for dual-frequency measurements. While difficult to implement, this established the potential for using ERCS and torso displacement for posture tracking.

In this letter, the subject data reported in the cited threshold-based sleep posture recognition study are analyzed in a new manner by integrating an optimizable ML approach to make the system autonomous, robust, and intelligent, as depicted in Fig. 1. Custom ML model uses a fixed hyperparameter, which is selected based on the grid search method [21]. Here, we present the Bayesian optimizable ML approach, which can update its parameter based on the dataset with environmental variations to produce the best results. The integration of optimizable ML classifiers provides a more effective single frequency categorized posture assessment, working without error for 86% of the subjects at 2.4 GHz, 78.3% at 5.8 GHz, and 98% using dual frequencies. Furthermore, the initial establishment of a supine position reference is not required, and this automated approach requires less computational time than the threshold approach [20].

Corresponding author: Shekh Md Mahmudul Islam (e-mail: [shekhs@hawaii.edu](mailto:shekhs@hawaii.edu)).

Associate Editor: Rolland Vida.

Digital Object Identifier 10.1109/LSENS.2022.3148378

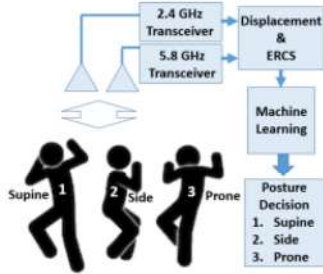


Fig. 1. Illustration of the proposed sleep posture recognition system. Torso displacement and ERCS derived from radar transceiver outputs are analyzed using optimizable ML classifiers to determine categorized posture as supine (face up), side, or prone (face down).

## II. THEORETICAL BACKGROUND

Radar cross section (RCS) is a measure of the magnitude of the wave reflected from a target and hence it is an indication of how detectable an object/target is with radar [19], [20]. The incident wave from the radar transmitter illuminates the torso surface of a human subject including the thorax and abdomen. During respiration, the contraction and relaxation of intercostal muscles act to change the volume of the thoracic cavity, which also causes the movement of the thorax and abdomen [20]. Additionally, when supine, the relaxed abdomen tends to be at a lower level than that of the thorax, which introduces a phase offset between the wave scattered from each part of the body [19]. The radar complex baseband signal is represented as

$$I_{BB} = A_T \cos \left[ \frac{4\pi}{\lambda} [x_H(t) + x_R(t)] + \phi_{tot} \right] + A_A \cos \left[ \frac{4\pi}{\lambda} [x_R(t - t_d)] + \phi_{tot} + \alpha \right] \quad (1)$$

and

$$Q_{BB} = A_T \sin \left[ \frac{4\pi}{\lambda} [x_H(t) + x_R(t)] + \phi_{tot} \right] + A_A \sin \left[ \frac{4\pi}{\lambda} [x_R(t - t_d)] + \phi_{tot} + \alpha \right] \quad (2)$$

where  $A_T$  and  $A_A$  are the amplitudes of the components from the thorax and abdomen, respectively,  $t_d$  is the time delay of the abdomen motion, and  $\alpha$  is the phase offset due to the difference in the nominal target range. While RCS measurements for fixed objects are proportional to the physical surface area, the area of interest when measuring respiratory displacements depends only on the portion of the body surface that moves with respiration. Reflections from clutter and stationary parts of the body do not contribute to this measurement; therefore, the measured RCS is described as the ERCS of the moving surface of the body [20]. With continuous respiration cycles, the overall body surface of human sleep postures directly affects the ERCS [20]. The captured baseband signal traces an arc on the complex  $I$ - $Q$  plot where the radius corresponds to the square root of the ERCS [20] and the length to displacement, which serve as “features” for posture determination.

## III. EXPERIMENTAL SETUP AND HUMAN SUBJECT STUDY

The Doppler radar system employed for the study was designed to extract two key respiratory measures, namely chest displacement and ERCS [10]. Signal generators were used to produce two different

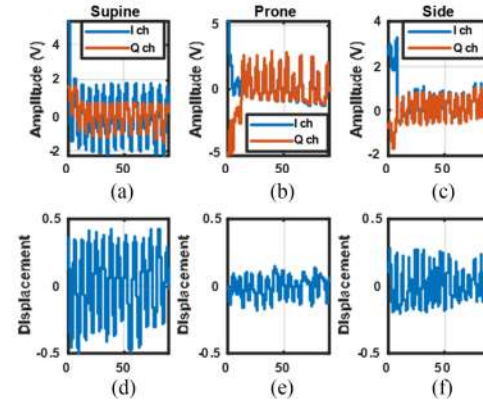


Fig. 2. Measured 2.4 GHz radar amplitude and displacement data for subject at 2 m. In-phase and quadrature data are shown for (a) supine, (b) prone, and (c) side postures, along with arc-tangent demodulated signals for (d) supine, (e) prone, and (f) side postures.

carrier frequencies, 2.4 and 5.8 GHz, to add diversity to the ERCS measurement. Low-frequency waves are most likely to satisfy the wave planarity condition of far-field measurement [20], whereas high frequencies result in more optical electromagnetic scattering where differences in size are more accurately detected [20]. The system had separate but identical transmitting and receiving antennas, two ASPPT2988 panel antennas for 2.4 GHz, and two-directional Wi-Fi antennas for 5.8 GHz. The experimental procedure involving human subjects was approved by an Institutional Review Board protocol number 14884. A total of 20 subjects, six females and 14 males, were included in the study. The mean and standard deviation of participant weight are 76.2 and 12.98 kg and heights are 174.05 and 9.09 cm, respectively. The body mass index varied from 19 to 31.8 kg/m<sup>2</sup>, where eight subjects had normal weight, 11 were overweight, and one was obese. For each subject, measurements were taken using three different recumbent postures.

## IV. RESULTS

### A. Feature Extraction

For each human subject, the radar baseband signal was recorded for 90 s in each posture and analyzed to find the relative ERCS and the absolute torso displacement. To extract features, the first 12 s were used for dc estimation and the next 39 s of the recorded time signal were segmented to produce a double testing dataset in the full respiration cycle. Fig. 2 illustrates the recorded 90-s datasets for three different postures along with the corresponding arc-tangent demodulated signals. Each segment traces an arc on the complex  $I$ - $Q$  plot where the radius is estimated using the center estimation algorithm [19], [20]. The square of the radius is proportional to the ERCS of the torso at the corresponding orientation. The angle scanned by the arc leads to the torso displacement magnitude during respiration. The ERCS variation occurs due to the different sizes of the subject, the curvature of the body surface, body fat, and respiration characteristics [11], [12]. Fig. 3 illustrates the ERCS variations in the  $I$ - $Q$  plot for three different postures using two different carrier frequencies. The radii for 2.4 GHz were 5.22, 15.72, and 3.4 V, and for 5.8 GHz were 2.63, 5.19, and 1.33 V, for supine, prone, and side postures, respectively.

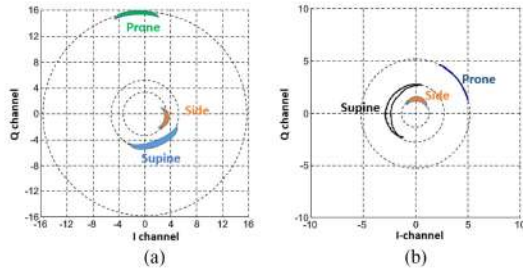


Fig. 3. Center-tracked *I*/*Q* arcs shown for subjects breathing in three sleep postures. Note that when prone, the subject presents the largest area of moving surface toward the radar antenna resulting in the largest radius.

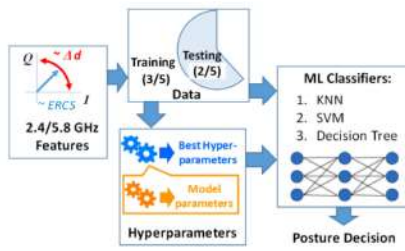


Fig. 4. Optimizable ML-based sleep posture recognition process.

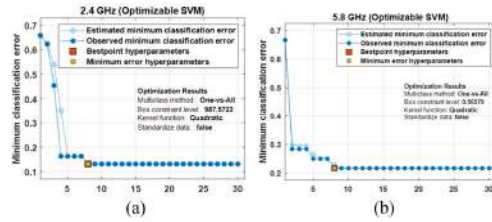


Fig. 5. SVM optimization for minimum classification error shown for (a) 2.4 GHz and (b) 5.8 GHz. Dark blue lines represent the minimum classification error and red squares represent the best hyperparameter (for minimum classification error).

### B. Optimizable ML Classifier and Hyperparameter Tuning

To evaluate the performance of different optimizable ML classifier algorithms, three different algorithms were integrated and tested using the Classification Learner App in MATLAB [21]. The approach is depicted in Fig. 4. The K-nearest neighbor (KNN) algorithm uses distance-based metrics, whereas the support vector machine (SVM) algorithm uses hyperplane-based approaches to classify [22]. The decision tree algorithm creates a decision tree of candidates on randomly selected data samples and selects the best decision tree using voting [22]. Initially, classification accuracy was assessed for data measured at a single frequency. The dataset was split into five parts whereby three-fifth of the data were used for training and two-fifth were used for testing. For hyperparameter tuning, Bayesian optimization with a box constraint level of 0.001–1000 was employed with 30 iterations for each classifier. A parameter box-constraint level of 76.7414 and 26.6629 produced the best performance for 2.4 and 5.8 GHz, respectively [21]. Fig. 5 illustrates the hyperparameter optimization curves that minimize the classification error with each iteration by utilizing different distance metrics for KNN (Euclidean, Hamming, etc.), kernel functions for SVM (linear, quadratic, Gaussian, etc.), and different split criteria for decision trees (towing rule, maximum deviance reduction, etc.) [21]. For 2.4 GHz, the SVM model with quadratic function

| 2.4-GHz            |       |         |         | 5.8-GHz            |       |         |         | Dual Frequency     |       |         |         |
|--------------------|-------|---------|---------|--------------------|-------|---------|---------|--------------------|-------|---------|---------|
| Estimated Postures |       | Overall |         | Estimated Postures |       | Overall |         | Estimated Postures |       | Overall |         |
| Supine             | Prone | Side    | Overall | Supine             | Prone | Side    | Overall | Supine             | Prone | Side    | Overall |
| 36                 | 3     | 2       | 40      | 90.0%              | 10.0% | 40      | 90.0%   | 10.0%              | 40    | 90.0%   | 10.0%   |
| 8                  | 31    | 0       | 85.0%   | 85.0%              | 15.0% | 40      | 80.0%   | 20.0%              | 40    | 80.0%   | 20.0%   |
| 4                  | 4     | 32      | 89.0%   | 89.0%              | 10.0% | 40      | 70.0%   | 30.0%              | 40    | 70.0%   | 30.0%   |
| 99.0%              | 85.0% | 20.0%   | 129     | 85.0%              | 15.0% | 129     | 80.0%   | 20.0%              | 129   | 80.0%   | 20.0%   |
| 10.0%              | 15.0% | 20.0%   | 10.0%   | 10.0%              | 10.0% | 10.0%   | 10.0%   | 10.0%              | 10.0% | 10.0%   | 10.0%   |
| Supine             | Prone | Side    | Overall | Supine             | Prone | Side    | Overall | Supine             | Prone | Side    | Overall |

(a) (b) (c)

Fig. 6. Confusion matrix for (a) 2.4 GHz, (b) 5.8 GHz, and (c) dual frequency test data. Accuracies of 85, 80.3, and 98.4% were attained for 2.4 GHz, 5.8 GHz, and dual-frequency assessments.

Table 1. Comparison of this work with the state of the art

| Approach                 | Radar Freq/Participants    | Computational Time | Accuracy (%)   |
|--------------------------|----------------------------|--------------------|--|
| [18] Custom ML           | FMCW 5.7–7.2 GHz 26 people | Not mentioned      | 94.1 % (Fixed environment only)                                |
| [20] Threshold           | CW 2.4/5.8 GHz 20 people   | 13 minutes         | 2.4 GHz: 78%<br>5.8 GHz: 65%<br>Dual: 100% (threshold adapted) |
| This work Optimizable ML | CW 2.4/5.8 GHz 20 people   | 1.37 minutes       | 2.4 GHz: 85%<br>5.8 GHz: 80%<br>Dual: 98.4%                    |

outperformed the other two classifiers with an accuracy of 85% and a minimum error of 0.15 [see Fig. 5(a)]. Similarly, for features extracted at 5.8 GHz, quadratic SVM superseded the other methods with an accuracy of 80.0% and a minimum classification error of 0.20 [see Fig. 5(b)]. The performance of different classifiers was also tested by analyzing combined dual-frequency extracted features. The decision tree algorithm with coarse function outperformed other classifiers with an accuracy of 98%. Fig. 6 shows the confusion matrix for the test datasets for 2.4 GHz, 5.8 GHz, and dual-frequency measurements. The matrix diagonal shows the correctly predicted postures, and classification accuracy calculated from the ratio of the correct prediction to the total number of predictions is also indicated. The combined frequency measurement produced better classification results likely due to the broad variations in ERCS and chest displacement [20].

### C. Comparison With the State of the Art

Table 1 illustrates the comparative analysis between the state-of-the-art techniques and the proposed approach. It clearly illustrates that the optimizable ML-based approach resulted in a more accurate and robust single-frequency decision algorithm (up to 13%) than the threshold technique and accuracy increased up to 5% over the custom ML approach. There is also a slight decrease in the accuracy of dual-frequency measurements from 100% down to 98%. It is expected that if these approaches are applied to additional subjects, beyond those used in the threshold determination study, the more robust optimizable ML technique would equal or surpass the threshold results. The computational time for decision-making of the proposed technique is approximately 1.37 min where feature extraction takes around 1.5 s and training takes around 81.18 s (Intel Core i7 8th Generation). In comparison, using the same processor threshold-based approach takes around 13 min for decision-making [20]. Furthermore, the reported threshold-based approach required supine position measurements to be observed and used as a calibration reference for ratio measurements taken with other postures [20]. The method proposed here does not require a calibration posture measurement. The optimizable ML-based classifier can learn after training for any posture measurements, making the system intelligent and automated. Since the proposed approach is based on subject-specific learning, the results validate the claim the method can effectively track sleep posture changes

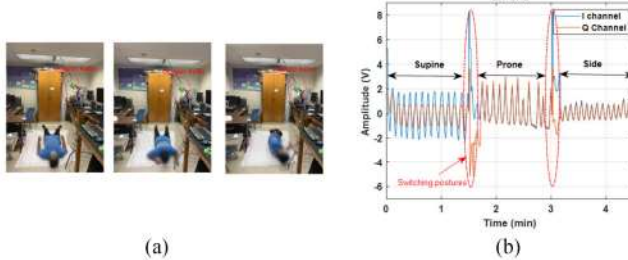


Fig. 7. (a) Experimental scenarios in an office environment. (b) Recorded data in time domain in an office environment. From [20].

throughout the night for a wide range of subjects. The data produced can be valuable for the assessment of sleep quality, tracking of compliance with prescribed sleep hygiene, and calibrating torso displacement according to posture for tracking of respiratory tidal volume [23], [24]. To test the efficacy of the optimizable ML approach to the custom ML approach with variation in an environment, we also experimented in an office environment. A 2.4-GHz Doppler radar was mounted on the ceiling and the subject reclined on a flat horizontal surface of 2.15 m shown in Fig. 7. A total of ten repetitive measurements were taken where the subjects started with supine position and then moved to prone and side postures. During switching position, there were abrupt spikes that were removed using the segmentation technique [20]. Similarly, any other abrupt changes during sleeping (movement of the legs, rolling, and fidgeting slightly) can also be removed using the segmentation technique. From the segmented portion, arc radius is calculated using center estimation and circle fitting algorithm [20]. From the arc radius and chest displacement measurement dataset using optimizable ML (Quadratic SVM), classifiers accuracy was around 84% where the best hyperparameter was obtained at box constraint levels of 75.84 and 24.52. On the other hand, using customized ML mode the accuracy was around 78%, which clearly illustrates that optimizable ML supersedes the performance of custom ML model with the change of the environment and the hyperparameter tuning also helps to achieve better accuracy as it can be tuned to produce the best output.

## V. CONCLUSION

A radar-based sleep posture recognition technique is proposed in this letter, which applies optimizable ML-based classifiers to ERCS and torso displacement measurements. The integration of optimizable ML classifiers with radar measurement increases the accuracy by 13% for single-frequency assessment and 6% for dual-frequency measurement. The proposed approach also reduced the computational time by almost 12 min. Further improvements such as integration of adaptive deep learning and implementing this system for multisubject scenarios by integrating signal processing approaches such as independent component analysis remain our future work to explore.

## ACKNOWLEDGMENT

This work was supported by U.S. National Science Foundation under Grant IIS1915738. This work involved human subjects or animals in its research. Approval of all ethical and experimental procedures and protocols was granted by the University of Hawaii Human Studies Program's Institutional Review Board (IRB), and performed in line with the CHS# 14884 "Remote Sensing of Physiological Motion Using Doppler Radar" protocol.

## REFERENCES

- [1] M. Kryger, T. Roth, and W. Dement, *Principles and Practice of Sleep Medicine*. Amsterdam, The Netherlands: Elsevier, 2017.
- [2] K. L. Knutson and E. Van Cauter, "Association between sleep loss and increased risk of obesity and diabetes," *Ann. New York Acad. Sci.*, vol. 1129, pp. 287–304, 2008, doi: [10.1196/annals.1417.033](https://doi.org/10.1196/annals.1417.033).
- [3] A. Oksenberg and D. S. Silverberg, "Avoiding the supine posture during sleep for patients with mild obstructive sleep apnea," *Amer. J. Respir. Crit. Care Med.*, vol. 180, no. 1, 2009, Art. no. 101, doi: [10.1164/ajrccm.180.1.101](https://doi.org/10.1164/ajrccm.180.1.101).
- [4] N. Goldberg, Y. Rodriguez-Prado, R. Tillery, and C. Chua, "Sudden infant death syndrome: A review," *Pediatr. Ann.*, vol. 47, no. 3, pp. e118–e123, 2018, doi: [10.3928/19382359-20180221-03](https://doi.org/10.3928/19382359-20180221-03).
- [5] H.-J. Lee, S.-H. Hwang, S.-M. Lee, Y.-G. Lim, and K.-S. Park, "Estimation of body postures on bed using unconstrained ECG measurements," *IEEE J. Biomed. Health Inform.*, vol. 17, no. 6, pp. 985–993, Nov. 2013.
- [6] S. Ostadabbas, M. Baran Pouyan, M. Nourani, and N. Kehtarnavaz, "In-bed posture classification and limb identification," in *Proc. IEEE Biomed. Circuits Syst. Conf.*, Lausanne, Switzerland, 2014, pp. 133–136.
- [7] T. Grimm, M. Martinez, A. Benz, and R. Stiefelhagen, "Sleep position classification from a depth camera using bed aligned maps," in *Proc. 23rd Int. Conf. Pattern Recognit.*, Cancun, Mexico, 2016, pp. 319–324.
- [8] J. Liu, X. Chen, S. Chen, X. Liu, Y. Wang, and L. Chen, "TagSheet: Sleeping posture recognition with an unobtrusive passive tag matrix," in *Proc. IEEE Conf. Comput. Commun.*, Paris, France, 2019, pp. 874–882.
- [9] T. Sakamoto, S. Mitani, and T. Sato, "Noncontact monitoring of heartbeat and movements during sleep using a pair of millimeter-wave ultra-wideband radar systems," *IEICE Trans. Commun.*, vol. E104-B, pp. 463–471, 2021, doi: [10.1587/transcom.2020EBP3078](https://doi.org/10.1587/transcom.2020EBP3078).
- [10] C. Li *et al.*, "A review on recent progress of portable short-range noncontact microwave radar systems," *IEEE Trans. Microw. Theory Techn.*, vol. 65, no. 5, pp. 1692–1706, May 2017.
- [11] A. D. Droitcour *et al.*, "Non-contact respiratory rate measurement validation for hospitalized patients," in *Proc. Annu. Int. Conf. IEEE Eng. Med. Biol. Soc.*, Minneapolis, MN, USA, 2009, pp. 4812–4815, doi: [10.1109/EMBS.2009.5332635](https://doi.org/10.1109/EMBS.2009.5332635).
- [12] S. M. M. Islam, O. Boric-Lubecke, and V. M. Lubecke, "Concurrent respiration monitoring of multiple subjects by phase-comparison monopulse radar using independent component analysis (ICA) with JADE algorithm and direction of arrival (DOA)," *IEEE Access*, vol. 8, pp. 73558–73569, Apr. 2020, doi: [10.1109/ACCESS.2020.2988038](https://doi.org/10.1109/ACCESS.2020.2988038).
- [13] M. Zakrzewski, A. Vehkaoja, A. S. Joutsen, K. T. Palovuori, and J. J. Vanhala, "Noncontact respiration monitoring during sleep with microwave Doppler radar," *IEEE Sensors J.*, vol. 15, no. 10, pp. 5683–5693, Oct. 2015.
- [14] F. Lin *et al.*, "SleepSense: A noncontact and cost-effective sleep monitoring system," *IEEE Trans. Biomed. Circuits Syst.*, vol. 11, no. 1, pp. 189–202, Feb. 2017.
- [15] M. Baboli, A. Singh, B. Soll, O. Boric-Lubecke, and V. M. Lubecke, "Wireless sleep apnea detection using continuous wave quadrature Doppler radar," *IEEE Sensors J.*, vol. 20, no. 1, pp. 538–545, Jan. 2020.
- [16] T. Rahman *et al.*, "DoppleSleep: A contactless unobtrusive sleep sensing system using short-range Doppler radar," in *Proc. ACM Int. Joint Conf. Pervasive Ubiquitous Comput.*, Osaka, Japan, 2015, pp. 39–50, doi: [10.1145/2750858.2804280](https://doi.org/10.1145/2750858.2804280).
- [17] F. Snigdha, S. M. M. Islam, O. Boric-Lubecke, and V. Lubecke, "Obstructive sleep apnea events classification by effective radar cross section (ERCS) method using microwave Doppler radar and machine learning classifiers," in *Proc. IEEE MTT-S Int. Microw. Biomed. Conf.*, Toulouse, France, Dec. 2020, doi: [10.1109/IM-BioC47321.2020.9385028](https://doi.org/10.1109/IM-BioC47321.2020.9385028).
- [18] S. Yue, Y. Yang, H. Wang, H. Rahul, and D. Katabi, "BodyCompass: Monitoring sleep posture with wireless signals," *Proc. ACM Interact., Mobile, Wearable Ubiquitous Technol.*, vol. 4, no. 2, pp. 1–25, Jun. 2020, doi: [10.1145/3397311](https://doi.org/10.1145/3397311).
- [19] J. E. Kiriazi, O. Boric-Lubecke, and V. M. Lubecke, "Dual-Frequency technique for assessment of cardiopulmonary effective RCS and displacement," *IEEE Sensors J.*, vol. 12, no. 3, pp. 574–582, Mar. 2012.
- [20] J. E. Kiriazi, S. M. M. Islam, O. Boric-Lubecke, and V. M. Lubecke, "Sleep posture recognition with a dual-frequency cardiopulmonary Doppler radar," *IEEE Access*, vol. 9, pp. 36181–36194, Feb. 2021, doi: [10.1109/ACCESS.2021.3062385](https://doi.org/10.1109/ACCESS.2021.3062385).
- [21] "Classification Learner," Accessed: Jan. 4, 2020. [Online]. Available: <https://www.mathworks.com/help/stats/classificationlearnerapp.html>
- [22] S. B. Kotsiantis, "Supervised machine learning: A review of classification techniques," *Informatica*, vol. 31, pp. 249–268, 2007.
- [23] W. Massagram, N. Hafner, V. Lubecke, and O. Boric-Lubecke, "Tidal volume measurement through non-contact Doppler radar with DC reconstruction," *IEEE Sensors J.*, vol. 13, no. 9, pp. 3397–3404, Sep. 2013.
- [24] O. Boric-Lubecke, V. Lubecke, A. D. Droitcour, B.-K. Park, and A. Singh, "Doppler radar physiological assessments," in *Doppler Radar Physiological Sensing*. Hoboken, NJ, USA: Wiley, 2016, pp. 171–206, doi: [10.1002/9781119078418.ch7](https://doi.org/10.1002/9781119078418.ch7).